

Nano-CNC Machining of sub-THz Vacuum Electron Devices

Diana Gamzina, *Member, IEEE*, Logan G. Himes, Robert Barchfeld, Yuan Zheng, Branko K. Popovic, Claudio Paoloni, EunMi Choi, and Neville C. Luhmann Jr., *Fellow, IEEE*

Abstract—Nano CNC machining technology is employed for the fabrication of sub-THz (100 – 1,000 GHz) vacuum electron devices. Sub-micron feature tolerances and placement accuracy have been achieved; surface roughness of a few tens of nanometers has been demonstrated providing high quality rf transmission and reflection parameters on the tested circuit structures. Details on the manufacturing approach is reported for the following devices: W-band sheet beam klystron, two designs of a 220 GHz sheet beam double staggered grating travelling wave tube, 263 GHz sheet beam travelling wave tube amplifier for an electron paramagnetic resonance spectrometer, 346 GHz sheet beam backward wave oscillator for fusion plasma diagnostics, 346 GHz pencil beam backward wave oscillator, and 270 GHz pencil beam folded waveguide travelling wave tube self-driving amplifier. Application of the Nano-CNC machining to nano-composite scandate tungsten cathodes as well as to passive rf components is also discussed.

Index Terms—High frequency, Micro-machining, Nano-CNC, Terahertz, Vacuum electron device

I. INTRODUCTION

MINIATURIZED vacuum electron devices (VEDs) promise high power and high efficiency at sub-terahertz frequencies (100 – 1000 GHz) if advanced manufacturing techniques are developed that not only address accuracy, and precision of manufacturing, but also produce excellent (<100 nm Ra) surface finishes and which are compatible with materials with good thermal and electrical properties. High

frequency vacuum electron devices find applications in communications [1], synthetic aperture radar [2], medical [3], biological [4], and plasma [5] imaging, material spectroscopy and processing [6].

Numerous Department of Defense and Department of Energy applications have long necessitated the development of high power rf VEDs that operate in the sub-terahertz region (0.1-1 THz). Slow wave devices that operate at these frequencies require microstructures on the order of microns to a few hundred microns, and tolerances of tenths to a few microns and with surface roughness constraint limits less than an rf skin depth (~ 70 nm at 1 THz) [1]. There are many approaches for the microfabrication of these devices, including Electric Discharge Machining (EDM) [7], Deep Reactive Ion Etching (DRIE) [8], and lithography methods (such as LIGA) [9], [10]. More recently, additive manufacturing (or 3D printing) techniques have also been under evaluation for fabrication of vacuum electronic devices [11], [12]. However, one technology that has been largely overlooked is computer numerical control (CNC) milling. The common wisdom has been that direct machining cannot meet the sensitive tolerances and surface roughness requirements of high frequency VEDs [13]. However, it has been shown [14]-[17] that Nano-CNC milling is a unique technology that can achieve the desired tolerances and surface finishes repeatedly, while also satisfying the stringent thermal and electrical conductivity constraints imposed when high power devices are desired. An average manufacturing time for a high frequency interaction structure using Nano-CNC milling is one month, which is comparable to or better than the development time needed for implementation of LIGA or DRIE techniques on a new interaction structure design.

Generous access to the DMG – Mori Seiki NN1000 Nano CNC mill has allowed the demonstration of tremendous progress in development of advanced VEDs. Over the past 7 years of Nano-CNC precision work, interaction structures for seven high frequency devices have been built. Furthermore, the resultant techniques have been applied to the machining of nano-composite scandate tungsten high current density cathodes [18], [21], optical mirrors and reflectors, high frequency transitions, couplers, and bends. Details on the manufacturing development of the interaction structures is reported: (1) 94 GHz sheet beam (SB) klystron circuit, (2) 220 GHz SB travelling wave tube (TWT) three-layer double staggered grating (DSG) circuit with overhead couplers, (3) 220 GHz SB TWT two-layer DSG circuit with in-line couplers, (4) 263 GHz SB TWT two layer DSG circuit, (5)

The manuscript was submitted on June 3, 2016. This work was supported by the U.K. EPSRC EP/L026597/1 Grant, DARPA Contract G8U543366, NSF MRI Grant CHE-1429258, DOE NSTX DE-FG02-99ER54518, DOD M67854-06-1-5118, and UNIST A17291. The authors would like to thank DMG Mori for their continued support and use of the NN1000 Nano CNC Machine. The authors would also like to thank previous members of the UC Davis millimeter wave research group: Anisullah Baig, Larry Barnett, Youngmin Shin, and Jianxun Wang.

D. Gamzina e-mail: dgamzina@ucdavis.edu, L. G. Himes e-mail: lghimes@ucdavis.edu, R. Barchfeld e-mail: rbarchfeld@ucdavis.edu, Y. Zheng email: zyzheng@ucdavis.edu, B. K. Popovic e-mail: bkpopovic@ucdavis.edu, N. C. Luhmann, Jr. e-mail: ncluhmann@ucdavis.edu; all above authors are with the Department of Electrical and Computer Engineering, University of California - Davis, Davis CA, 95616, USA. C. Paoloni email: c.paoloni@lancaster.ac.uk, he is with the Engineering Department, Lancaster University, Lancaster, United Kingdom. E. Choi email: emchoi@unist.ac.kr, she is with the Department of Physics & School of Electrical and Computer Engineering, Ulsan National Institute of Science and Technology, Ulsan, South Korea

346 GHz SB backward wave oscillator (BWO) DSG circuit, (6) 346 GHz pencil beam BWO double corrugated waveguide (DCW) circuit, and (7) 270 GHz pencil beam TWT folded waveguide (FW) circuit. These devices were tested with the Davis Millimeter Wave Research Center state-of-the-art millimeter wave vector network and spectrum analysis test equipment operating up to 350 GHz.

II. EQUIPMENT AND TOOLING

A. Background on Nano-CNC Milling Machine

The NN1000 DCG HSC [19] nano-CNC milling machine was developed by Digital Technology Laboratory, subsidiary of DMG – MORI, in Davis CA as a prototype machine for advancement of nano-precision manufacturing capabilities. This 5 axes prototype machine has a movement position accuracy of 1 nm / 100 mm and a repeatability of 5 nm / 100 mm. These accuracies are achieved by the use of air bearings on all axes, linear servos and laser scales for movement and position feedback, a high rotation per minute (RPM) air spindle, and the control system developed by DMG-Mori. The spindle currently employed in the machine has a maximum speed of 50,000 RPM with other options allowing spindle speeds up to 160,000 RPM. The high precision systems of the NN1000 working in concert provide us with the ability to make fine microstructures as well as complex three-dimensional features using mechanical removal techniques at a scale that is difficult to achieve by other mechanical machining methods.

B. Tooling

Additionally, the NN1000 Nano-CNC machine has tooling features that provide expanded usability (see Fig. 1 (a)). The NN1000 is capable of not only rotary milling but also scribing (similar to shaper techniques) and turning, which is advantageous when making high precision parts with difficult geometries. These various material removal processes in addition to machine accuracy means the downstream precision of the tooling plays a significant role in the quality and performance of the finished VEDs. Given this, considerable research was conducted to find tooling that performed to a level suitable for use on the NN1000 machine. Our tooling can be divided into two categories, coated carbide and diamond tooling. The carbide tooling is of the micro-grain type and has been employed for tools down to 76 μm in diameter [17]. The tooling performance was also investigated with respect to different high performance coatings including AlTiN (Titanium aluminum nitride), CBN (cubic boron nitride), and polycrystalline diamond to name just a few. These coatings significantly affect the lifetime utility of the tools and facilitate the production of small features with good surface roughness. The diamond tooling we utilize is both of the end mill/rotary type and fixed turning/scribing type. Both of these types of tools have utilized monocrystalline and polycrystalline diamonds, affixed to a shank or tooling insert depending on the process. The diamond tooling shows little to no wear and has achieved surface roughness averages (R_a) of less than 50 nm over the entire surface of a part. Scribing with a 90° diamond insert has allowed us to create other unique parts, such as diffraction gratings and pyramidal reflecting arrays,

which are useful for research at terahertz region frequencies. In addition to the tools noted in [17], the tools shown in Fig. 1 are also employed during circuit manufacturing on the NN1000.



Fig. 1. Tooling used on NN1000: (a) Brazed diamond facing mill, (b) 0.3046 mm diameter bull nose end-mill, (c) 0.076 mm diameter end mill show next to a human hair

C. Fixturing

Fixturing plays a key role in the development of a high performance and precision manufacturing regimen for high frequency devices. Often work holding and fixturing is overlooked in the development of micro- and nano- scale devices; however, we have found that part fixturing is of the utmost importance in the micro and nano machining processes. We have discovered that properly engineered work holding leads to more accurate small scale features, decreases machining time, and reduces the inaccuracies inherent in tool and machine changing processes. The fixturing is also designed to reduce part position errors due to mechanical and thermal discrepancies using Finite Element Analysis. A model of the fixturing and the 346 GHz BWO cold test circuits is shown in Fig. 2 (b), whereas Fig. 2 (c) shows the completed 346 GHz cold test circuits mounted on the fixturing. A “unitized” part holding system is also implemented, allowing for different part designs to use the same jig as well as for fixturing multiple parts at the same time. Work holding developed at UCD has been responsible in reducing the time of surfacing processes by > 60% and has improved the accuracy and repeatability of production of rf circuits for VEDs.

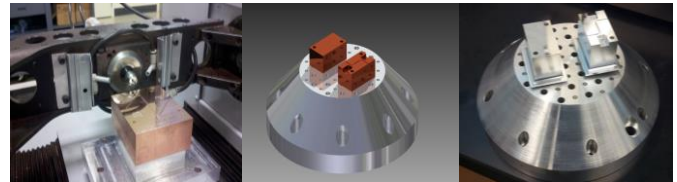


Fig. 2. (a) Machining of the flanges on the compact 220 GHz SB DSG Circuit, (b) Solid model of the fixturing for the 346 GHz BWO DCW circuit, (c) Completed cold test structure of the 346 GHz BWO DCW circuit

III. INTERACTION STRUCTURES OF HIGH FREQUENCY DEVICES

A. 94 GHz SB Klystron Circuit

The W-band (94 GHz) sheet beam klystron (WSBK) designed and developed at UC Davis [22][23][24] featured a 12.5: 1 aspect ratio sheet electron beam and 8-cavity interaction structure demonstrating 56 kW in short pulse and 10 kW in long pulse operation modes. The final circuit structure used for device demonstration was manufactured using commercially available conventional high-speed CNC milling techniques. Nano CNC milling was evaluated for feasibility during the development stage of the device, but later discounted as a final fabrication option due to excessively

long (~3 months) manufacturing time required for the 6.5 in by 4 in circuit area. DLC (diamond like coated) 0.4572 mm diameter carbide tools were used for machining of the circuit cavities and diamond scribing (see Fig. 3 (a)) was implemented for machining of the top mating surface. Surface roughness of 115 nm R_a was achieved on the internal surfaces of the cavities (note that the skin depth at 94 GHz is 210 nm), see Fig. 3 (b) and (c), surface roughness of <40 nm was achieved on the top mating surface.

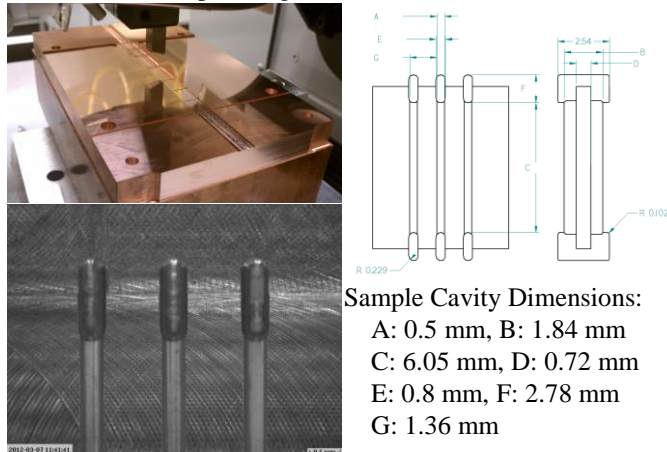


Fig. 3. (a) WSBK being machined by the NN1000 CNC mill, (b) Three-gap cavity micrograph, (c) Sample three-gap cavity model and dimensions.

B. 220 GHz SB TWT Three-Layer DSG Circuit with Overhead Couplers

The G-band sheet beam wide bandwidth TWT was designed and demonstrated under the DARPA HiFIVE program by a team from Teledyne Scientific, UC Davis, and CPI [25][26]. The TWT amplifier provided over 30 dB of gain in high gain operation mode with 6.5 GHz of bandwidth and over 25 dB of gain in wide bandwidth operation mode with 20 GHz of bandwidth; 114 W of rf output power was measured at 201.5 GHz. The DSG circuit used in this device was fabricated in a three layer mode which were then diffusion bonded to create the full circuit structure. The bottom structure (see Fig. 4 (a) and (f)) contained the lower circuit cavities as well as the beam tunnel, the middle layer (0.472 mm thick, see Fig. 4 (b) and (e)) contained the upper circuit cavities featuring through cutouts for connections to the couplers, and the top layer (see Fig. 4 (c)) included the overhead input, output, and sever coupler structures (see Fig. 4 (h)) and waveguides. The diffusion bonded circuit structure (see Fig. 4 (d)) was then cold tested to verify the circuit's performance [26] and then outside machined into the desired shape (see Fig. 4 (g)) for incorporation into the vacuum envelope of the tube. DSG circuit dimensions shown on Fig. 4 (i) were: A=0.152 mm, B=0.796 mm, C=0.320 mm, D=0.350 mm, and E=0.468 mm. Surface roughness of 96 nm R_a was achieved on the circuit cavities; the mating surfaces were milled instead of scribed and 55 nm R_a was achieved. The tools used for manufacturing include 0.254 mm AlTiN coated carbide tools and monocrystalline diamond surfacing and scribing tools. Due to the compactness of the design, rectangular alignment features was employed having 2 μ m maximum material

condition clearance; 0.0625 in pin holes were employed for aligning the coupler structures.

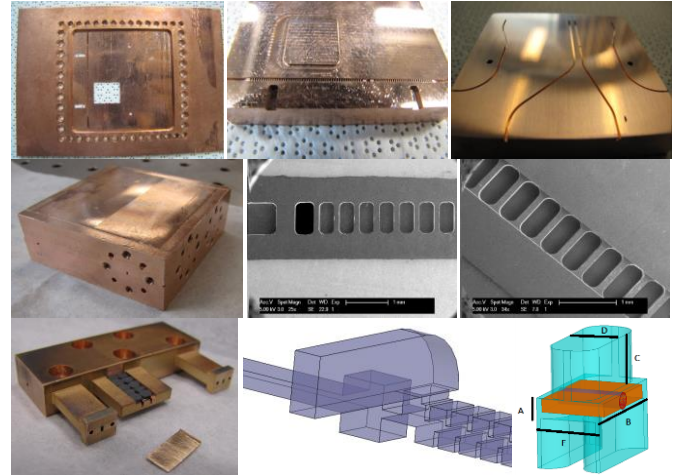


Fig. 4. (a) Middle layer of the circuit structure, (b) Bottom layer of the circuit structure, (c) Top layer of the circuit assembly with input, output, and sever waveguides, (d) Fully assembled and diffusion bonded three-layer circuit structure with three out of four WR-4 waveguide outputs visible, (e) SEM image of the middle circuit layer showing the cutout machined through the material thickness, (f) EM model of the overhead coupler design, (g) Circuit structure shown in (d) after outside machining operation, (h) Overhead coupler design, (i) DSG circuit's unit cell

C. Compact 220 GHz SB TWT Two-Layer DSG Circuit with In-Line Couplers

The DARPA HiFIVE TWT described in the section above was designed to operate in a permanent solenoidal magnet [27], which weighs over 200 lbs. To demonstrate that a compact version of the device is feasible, the design was modified to use a periodic cusped magnetic (PCM) structure for beam confinement. A TWT designed in this manner would be about 6 in long and weigh about 5 pounds. The dimensions of the DSG circuit were very similar to the original HiFIVE design. Two circuit halves (see Fig. 5 (a)) were manufactured and diffusion bonded together at which point cold circuit transmission and reflection parameters were evaluated [28][29]. The diffusion bonded assembly was then outside machined to provide pockets for the PCM structure as well as flanges for the electron gun, rf windows, and collector (see Fig. 5 (c)). Note that mating surfaces for the electron gun and window flanges were machined at the same time as the circuit itself on the NN1000 providing submicron placement accuracy between critical features. Even though this design is more compact overall, it provides significantly more room for couplers and alignment features in the center plane between the PCM magnets. Additional information on the in-line coupler design can be found in [30][31]. The manufacturing tools include 0.3048 mm \varnothing AlTiN and polycrystalline diamond coated carbide end mills as well as monocrystalline diamond surfacing tools. Surface roughness of 74 nm R_a was obtained in the circuit cavities (see Fig. 5 (b)); the mating surfaces between circuit halves were milled and surface roughness of 40 nm was obtained.

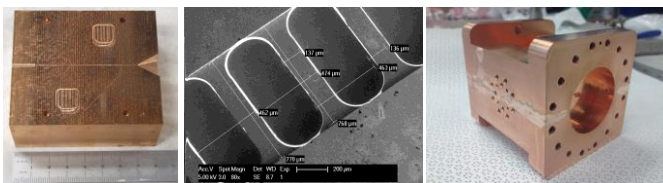


Fig. 5. (a) 220 GHz DSG circuit half, (b) SEM image of the compact version of the DSG circuit, (c) Diffusion bonded and outside machined TWT structure including the DSG circuit inside

D. 263 GHz SB TWT Two-Layer DSG Circuit

As part of the 263 GHz TWT amplifier development for an electron paramagnetic resonance spectrometer [32][33] system funded under the NSF MRI program, a DSG double layer cold test circuit has been fabricated, diffusion bonded, and tested. The layout of the full circuit is shown in Fig. 6 (a) and the diffusion bonded cold test structure is shown in Fig. 6 (b).

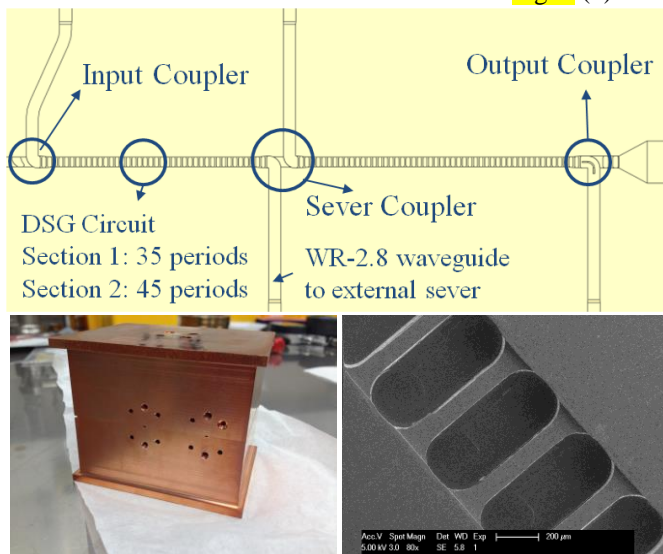


Fig. 6. (a) The full layout of the 263 GHz DSG circuit half, (b) Diffusion bonded cold test structure including the DSG circuit inside, (c) SEM image of the 263 GHz circuit

The results were reported in [32] showing around 5 dB loss and a 15 dB transmission window over 25 GHz of bandwidth. The tools used for manufacturing include 0.254 mm \varnothing AlTiN, CBN, polycrystalline diamond coated carbide end-mills. Surface roughness of 100 nm R_a was achieved on circuit cavities (see Fig. 6 (c)), the mating surfaces of the two halves were diamond scribed to achieve 50 nm R_a surface finish; and four 0.125 in pin holes were used for alignment.

E. 346 GHz SB BWO DSG Circuit

Currently, an optically pumped 693 GHz far-infrared laser based scattering system is being developed for the NSTX-U magnetic confinement device for micro-turbulence analysis [34][35]. The scattered radiation is detected with a 4-pixel subharmonic heterodyne receiver mixer array using a VDI multiplier to provide the LO power. Future plans envision expansion to 16-pixels which necessitates the development of a high power BWO [36][37][38][39]. To satisfy this need, a 1 W continuous wave 346 GHz SB BWO is being developed in a collaborative effort between UC Davis, Lancaster University, and Beijing Vacuum Electronics Research Institute to provide a compact local oscillator source for pumping the subharmonic receiver mixer array. One of the two parallel

approaches uses a 65-cell DSG circuit with the following dimensions (see Fig. 4 (i)): $A=0.090$ mm, $B=0.483$ mm, $C=0.170$ mm, $D=0.141$ mm, $E=0.185$ mm, and a SB electron gun featuring nano-composite scandate tungsten cathode with 92 A/cm² beam current density loading. The solid model of the device, manufactured cold test circuits, and the SEM image of the circuit cavities are shown in Fig. 7. The first cold test circuit was manufactured in aluminum and gold plated to enhance the transmission performance parameters, results were reported in [38] and suffered more than 10 dB of insertion loss across the transmission band. The poor performance is attributed to the surface roughness of 200-400 nm R_a on the circuit's cavities. Tools of 0.127 mm \varnothing in size were used for manufacture of this circuit.



Fig. 7. (a) 346 GHz compact BWO shown with 6 in ruler for scale, (b) The cold test circuit structures, (c) SEM image of the DSG circuit cavities

F. 346 GHz Pencil Beam BWO DCW Circuit

In parallel with the above described effort, a pencil beam based device combined with a DCW [40] circuit is being developed for demonstration of 1 W continuous wave power at 346 GHz [30]. A cold test circuit was also manufactured in aluminum and poor surface roughness quality was also observed ($R_a \sim 200$ -400 nm). The tools employed in this circuit were \varnothing 0.076 mm micro-grain carbide tools, smallest ever to be employed on the NN1000 machine. The features manufactured using these small diameter tools had worse surface finish than the ones machined with larger tools. This can be attributed to the significant increase in 0.076 mm diameter tool deflection (up to 3 times when compared to the \varnothing 0.127 mm tools) due to the reduced tool stiffness. The DCW circuit design features a simple pillar structure surrounding the electron beam tunnel that can be machined on just one circuit half allowing the second circuit half to be flat and serve as a cover. Dimensions of the manufactured structure are (see Fig. 8 (c)): $A=0.060$ mm, $B=0.120$ mm, $C=0.140$ mm, $D=1.5$ mm, $E=0.200$ mm.

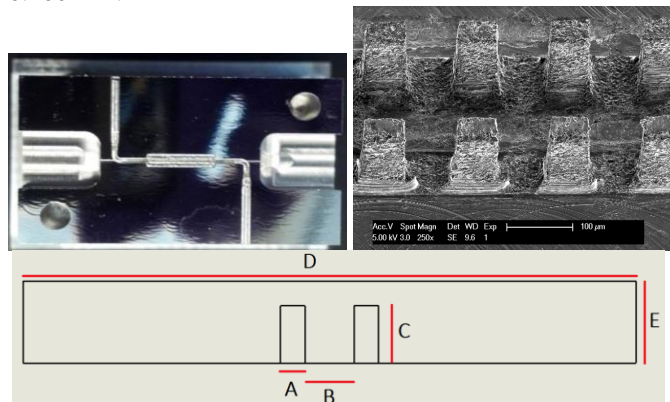


Fig. 8. (a) 346 GHz DCW cold test circuit, (b) SEM image of the circuit pillars, (c) Dimensions of the DCW circuit structure

G. 270 GHz Pencil Beam TWT FW circuit

In a collaboration between Ulsan National Institute of Science and Technology and UC Davis, an ultra-compact pencil beam 270/410 GHz folded wave travelling wave tube amplifier integrated with an extended interaction oscillator driver is under development [41]. The circuit features an 0.136 mm wide and 0.681 mm deep waveguide meandering with 0.344 mm period that is 0.591 mm wide; the beam tunnel diameter is 0.180 mm, see Fig. 9 (b). Tools of \varnothing 0.076 mm with 3:1 aspect ratio were used to manufacture the cold test structure shown in Fig. 9 (a). Surface roughness of 163 nm R_a was achieved on the waveguide surfaces. The two circuit halves were machined into a single copper block to reduce time needed for the machining of the top mating surface, the block is cut in half using electric discharge machining to create upper and lower circuit halves. The high aspect ratio (9.5:1) 0.036 mm wide pillars have burrs that are difficult to remove due to fragility of the pillars, see Fig. 9 (c).



Fig. 9. (a) Cold test structure of the 270 GHz FW circuit, (b) Model of the FW circuit with circular beam tunnel, (c) SEM image of the Nano-CNC machined FW circuit structure

IV. SUB-COMPONENTS FOR VEDS

A. Nano-Composite Scandate Tungsten Cathodes

Nano-composite scandate tungsten cathodes have been demonstrated to have superior performance when compared to commercially available ones [21], [42], [43]. Integration of these cathodes into VEDs requires machining of the prepared pellet into the desired shape [44], [45]. It was found that Nano-CNC machining not only provides the best dimensional accuracy, but it also produces the most optimal emission surface conditions. Fig. 10 (a) shows an image of the emission surface machined using the NN1000, whereas Fig. 10 (b) and (c) show images of the smudged emission surfaces machined using 2,500 RPM turning operations with varying feed rates. Smudged pores will restrict barium resupply to the emission surface and hinder the enhanced performance of the nano-structured cathode. Furthermore, Nano-CNC milling can achieve few hundred nanometer surface roughness average (see Fig. 10 (d), (e)), which is essential to achieving the desired velocity spread at the surface of the emitter.

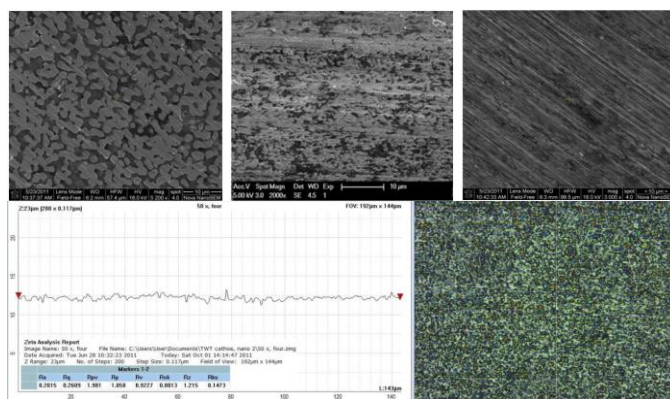


Fig. 10. (a) Cathode emission surface machined using NN1000 at 50,000 RPM, (b) and (c) Partially and fully smudged cathode emission surfaces, respectively, (d) Surface roughness analysis of the cathode emission surface, (e) Optical microscope image of the emission surface used for surface roughness analysis

B. Passive RF Components

High precision machining is also essential for the manufacture of passive rf components; they commonly require similar tolerances and surface roughness conditions as the high frequency interaction structures themselves. Three example structures are discussed here; see Fig. 11. The infrared diffraction grating was manufactured using a 90° diamond scribe producing 3.3 micron deep and 6.7 micron wide triangular grooves. The quasi-optical (QO) W-band H-bend was machined in two halves and then diffusion bonded together to create the overmoded waveguide (6.8 mm x 2.54 mm) structure. The G-band power combiner (1.092 mm x 0.546 mm) was also machined in two halves and diffusion bonded together. Surface roughness average of less than 200 nm was achieved on all of these components.

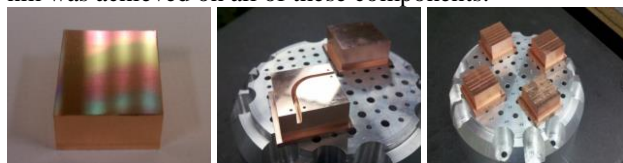


Fig. 11. (a) Infrared diffraction grating, (b) QO W-band H-bend, (c) G-band power combiner

V. SUMMARY

Nano-CNC machining technology allows for significant advancement in development of high frequency vacuum electronics allowing one to achieve desired sub-micron tolerances and surface roughness quality of less than the skin depth. Proper material, tooling, fixturing, and machine setting selection can promise high quality results, but still significant advancement in tooling technology is needed for nano-CNC machining to produce desired results at frequencies of 300 GHz and above. Also, production times with nano-CNC machining can compete with other manufacturing techniques when building devices for frequencies between 100 GHz and 300 GHz, but they are much too slow for low frequency and terahertz frequency devices.

Qualitative comparison of manufacturing methods suitable for high frequency vacuum electron device fabrication was reported in [10]. UV LIGA and DRIE techniques have similar performance parameters to Nano-CNC milling, but can be

more cost-effective in large scale production after process development completion. Electric discharge machining can be a good alternative to Nano-CNC milling if metal polishing techniques are advanced to achieve nano-scale surface roughness. Furthermore, additive manufacturing promises significant advancement for vacuum electronics technology, but considerable progress is needed to improve quality of copper, density, accuracy, and surface roughness.

REFERENCES

- [1] R. N. Simons, et al., "Demonstration of multi-Gbps data rates at Ka-band using software-defined modem and broadband high power amplifier for space communications," in *Microwave Symposium Digest (MTT), 2011 IEEE MTT-S International*, pp.1-4, 2011
- [2] H. B. Wallace, "Video Synthetic Aperture Radar (ViSAR) DARPA" April 30, 2012
- [3] F. Sterzer, "Microwave medical devices," *IEEE Microwave Mag.*, vol. 3, no. 1, pp. 65-70, 2002
- [4] A. Schweiger, G. Jeschke, Principles of Pulse Electron Paramagnetic Resonance, Oxford: University Press, 2001
- [5] D.R. Smith, et al., "A collective scattering system for measuring electron gyroscale fluctuations on the National Spherical Torus Experiment," *Review of Scientific Instruments*, 79, 123501, 2008
- [6] Miyake, Shoji, "Millimeter-wave materials processing in Japan by high-power gyrotron," in *Plasma Science, IEEE Transactions on*, vol.31, no.5, pp.1010-1015, Oct. 2003
- [7] R. L. Ives, "Microfabrication of high-frequency vacuum electron devices," in *IEEE Transactions on Plasma Science*, vol. 32, no. 3, pp. 1277-1291, June 2004.
- [8] Basten, M.A. et al., "233-GHz High-Power Amplifier Development at Northrop Grumman," XVII International Vacuum Electronics Conference, 2016
- [9] C. D. Joye et al., "Demonstration of a high power, wideband 220 GHz serpentine waveguide amplifier fabricated by UV-LIGA," *Vacuum Electronics Conference (IVEC), 2013 IEEE 14th International*, Paris, 2013, pp. 1-2.
- [10] Baig, A., et al., "Design, Fabrication and RF Testing of Near-THz Sheet Beam TWTA," *Terahertz Science and Technology*, Vol. 4, No. 4, pp. 181-207, 2011
- [11] P. Frigola, O.A. Harrysson, T.J. Horn, et al., "Fabricating Copper Components with Electron Beam Melting," *Advanced Materials and Processes*, pp. 20-24, July 2014.
- [12] A. D. Andreev, M. K. Peterson Lach, and J. G. Moxness, "3D Printing and Additive Manufacturing of Advanced Slow-Wave Structures for Millimeter-Wavelength and Terahertz-Frequency High-Power Vacuum Electronic Slow-Wave Devices," Technical Report # RMS-5111, Raytheon Missile Systems, approved for public release on June 26, 2013
- [13] Gamzina, D., et al., "Nanoscale surface roughness effects on THz vacuum electron device performance," in *IEEE Transactions on Nanotechnology*, Vol. 15, No. 1, 2015
- [14] Gamzina, D., et al., "Nano CNC milling technology for terahertz vacuum electronic devices," in *IEEE International Vacuum Electronics Conference (IVEC)*, pp.345-346, 2011
- [15] Barchfeld R., et al., "Nano CNC milling of two different designs of 0.22 THz TWT circuits," in *IEEE International Vacuum Electronics Conference (IVEC)*, pp. 549-550, 2012
- [16] Baig, A., et al., "Simulation analysis of nano-CNC fabricated 220 GHz ultra wide band TWTA," in *IEEE Thirteenth International Vacuum Electronics Conference (IVEC)*, pp.393-394, 2012
- [17] Himes, L., et al., "Development of Nano Machining Techniques to Bridge the Terahertz Gap," in *IEEE International Vacuum Electronics Conference (IVEC)*, 2016
- [18] Busbahr, D., et al., "Effects of Thermal Processing and Machining on Emission Surface Quality of Nano-Composite Scandate Tungsten Cathodes," *IEEE International Vacuum Electronics Conference (IVEC)*, 2016
- [19] Mori Seiki Co., Ltd, "Brochure of NN1000 DCG HSC," 2011
- [20] Okwudire, C. E. and J. Lee, "Optimal Motor Location for the Reduction of Residual Vibrations in Mode-Coupled Ultra-Precision Manufacturing Machine," *ASME 2013 International Manufacturing Science and Engineering Conference*, Vol.2, 2013
- [21] Zhao, J., et al., "Scandate Dispenser Cathode Fabrication for A High-Aspect-Ratio High-Current-Density Sheet Beam Electron Gun," in *IEEE Transactions on Electron Devices*, Vol. 59, No. 6, pp. 1792-1798, 2012
- [22] Wang, J., et al., "Electron Beam Transport Analysis of W-band Sheet Beam Klystron," *Physics of Plasmas*, Vol. 17, 2010
- [23] Shin, Y., et al., "Particle-In-Cell (PIC) Simulation Analysis of a Quasi-Optical W-Band Sheet Beam Klystron," *IEEE Transactions on Electron Devices*, Vol. 58, 2011
- [24] Shi, Z., et al., "3-D Simulations and Design of Multistage Depressed Collectors for Sheet Beam Millimeter Wave Vacuum Electron Devices," in *IEEE Transactions on Electron Devices*, vol.60, no.9, pp.2912-2917, 2013
- [25] Field, M., et al., "Development of a 220 GHz 50 W sheet beam travelling wave tube amplifier," in *IEEE International Vacuum Electronics Conference (IVEC)*, pp. 225-226, 2014
- [26] Baig, A., et al., "0.22 THz wideband sheet electron beam traveling wave tube amplifier: Cold test measurements and beam wave interaction analysis," *Physics of Plasmas*, Vol. 19, 2012
- [27] Stockwell B.C., et al., "P4-2: Permanent magnet for HiFIVE sheet beam transport," *IEEE International Vacuum Electronics Conference (IVEC)*, pp. 451-452, 2010
- [28] Baig, A., et al., "MEMS compatible sever for 220 GHz ultra wide band twta: design and particle-in-cell analysis," *Progress In Electromagnetics Research Letters*, Vol. 41, 135-148, 2013.
- [29] Baig, A., et al., "233 GHz ultra-wide band TWTA: PPM Integrated sheet electron beam transport and PIC analysis," in *2013 38th International Conference on Infrared, Millimeter, and Terahertz Waves (IRMMW-THz)*, pp.1-2, 2013
- [30] Baig, A., et al., "Simulation analysis of nano-CNC fabricated 220 GHz ultra wide band TWTA," in *IEEE Thirteenth International Vacuum Electronics Conference (IVEC)*, pp.393-394, 2012
- [31] Baig, A., et al., "Sever design and full model particle-in-cell simulation analysis for a 220 GHz ultra wideband TWTA," in *2011 36th International Conference on Infrared Millimeter and Terahertz Waves (IRMMW-THz)*, pp. 1-2, 2011
- [32] Zheng, Y., et al., "Design of a Compact and High Performance 263 GHz SB-TWT Circuits," *IEEE International Vacuum Electronics Conference (IVEC)*, 2016
- [33] Zheng, Y., et al., "Design of an Edge Band Stable Sheet Beam TWT Slow Wave Circuit," *Transaction on Electron Devices*, manuscript submitted for publication
- [34] S.M. Kaye et al, "An over view of recent physics results from NSTX," *Nuclear Fusion*, Vol. 55, 104002, 2015.
- [35] Barchfeld, R., et al., "High-k Scattering and FIRE TIP Diagnostic Upgrades for NSTX-U", *57th Annual Meeting of the APS Division of Plasma Physics*, Vol. 60, No. 19, 2015.
- [36] Paoloni, C., et al., "THz Backward-Wave Oscillators for Plasma Diagnostic in Nuclear Fusion," in *IEEE Transactions on Plasma Science*, vol. 44, no. 4, pp. 369-376, April 2016.
- [37] Paoloni, C., et al., "Magnetic fusion energy plasma diagnostic needs novel THz BWOs," *IEEE International Vacuum Electronics Conference (IVEC)*, 2015
- [38] Popovic, B., et al "Design and fabrication of a sheet beam BWO at 346 GHz," in *Vacuum Electronics Conference (IVEC)*, 2015 *IEEE International*, 2015
- [39] Popovic, B., et al., "346 GHz BWO for fusion plasma diagnostics," *2014 39th International Conference on Infrared, Millimeter, and Terahertz waves (IRMMW-THz)*, Tucson, AZ, 2014
- [40] M. Mineo, et al., "Double-Corrugated Rectangular Waveguide Slow-Wave Structure for Terahertz Vacuum Devices," *IEEE Transactions on Electron Devices*, vol. 57, no. 11, pp. 3169-3175, Nov. 2010.
- [41] Lee, I., et al., "Design Study of an Energy-Recirculating G-band Self-driving Folded Waveguide Travelling Wave Tube," *IEEE International Vacuum Electronics Conference (IVEC)*, 2016
- [42] Liang, W., "DC Emission Characteristic of Nanosized-Scandia-Doped Impregnated Dispenser Cathodes," in *IEEE Transactions on Electron Devices*, vol. 61, no. 6, pp. 1749-1753, June 2014.
- [43] Vancil, B., "Scandate Dispenser Cathodes With Sharp Transition and Their Application in Microwave Tubes," in *IEEE Transactions on Electron Devices*, vol. 61, no. 6, pp. 1754-1759, June 2014.
- [44] Yang, F., "Investigation of Nanosized-Scandia-Doped Dispenser Cathodes With Machined Surfaces," in *IEEE Transactions on Electron Devices*, vol. 63, no. 4, pp. 1728-1733, April 2016

[45] Busbaher, D., "Effects of Thermal Processing and Machining on Emission Surface Quality of Nano-Composite Scandate Tungsten Cathodes," *2016 IEEE International Vacuum Electronics Conference (IVEC)*, 2016

Diana Gamzina, B.S. (2008, UC Davis) with a double major in Mechanical Engineering and Materials Science; M.S. (2012, UC Davis) in Mechanical Engineering on nano-composite scandate tungsten cathodes; Ph.D. (2016, UC Davis) in Mechanical and Aerospace Engineering on thermo-mechanical design and analysis of high frequency and high power vacuum electron devices. She has been a staff development engineer at the UC Davis millimeter-wave research group since 2008. Her expertise include developing new technologies in high frequency vacuum electronics, micro and nano scale fabrication techniques, high current density thermionic cathodes, diffusion bonding and brazing of assemblies for ultrahigh vacuum environments, thermo-mechanical design and analysis, high heat flux materials, and operation.

Logan Himes, B.S. 2010 from UC Davis in Biotechnology and Applied Microbiology, and joined the UC Davis millimeter-wave research group in 2011. He specializes in the precision fabrication of millimeter wave components and assemblies using the latest in manufacturing techniques. His manufacturing skills include: micro- and nano- machining methods for miniature parts, CNC/CAM controls for high speed/high accuracy part manufacture, design and CAD modeling, Finite Element Analysis, precision measuring and quality control. He possesses 15 years of standard machining experience, 10 years of CNC machining experience, and 4 years of nano-CNC machining experience.

Robert Barchfeld, B.S. 2009 from Sacramento State University in physics, summa cum laude. He joined the millimeter-wave and microwave research group in the department of applied science in Fall of 2010 as a Ph.D. student. His interests include studying plasma physics, fusion, and millimeter-wave optics.

Yuan Zheng, B.S. 2010 in vacuum electronics from the University of Electronic Science and Technology of China, Chengdu, China, where he is currently working toward the Ph.D. degree. He joined the UC Davis millimeter wave research group in 2014 as a visiting scholar. His current research concentrates on high-power millimeter-wave devices, including SB TWTs and SB klystrons.

Branko Popovic, B.S. 2011 from the University of Iowa in Electrical Engineering. He joined the millimeter-wave and microwave research group at UC Davis in 2011 as a Ph.D. student. His research interests are RF and Microwave circuits.

Claudio Paoloni, (M'86–SM'11) received the Laurea degree in electronics engineering from the University of Rome Sapienza, Rome, Italy, in 1984. He has been a Professor of Electronics with the Department of Engineering, Lancaster University, Lancaster, U.K., since 2012, where he is currently the Head of the Engineering Department.

EunMi Choi, (S'03–M'14) received the B.S. degree in physics from Ewha Womans University, Seoul, South Korea, in 2000, the M.S. degree in physics from POSTECH, Pohang, South Korea, in 2002, and the Ph.D. degree in physics from Massachusetts Institute of Technology, Cambridge, MA, USA, in 2007. Currently, she is an Associate Professor with the Physics Department and School of Electrical and Computer Engineering at Ulsan National Institute of Science and Technology (UNIST), Ulsan, South Korea, where she joined as an Assistant Professor in 2010. Her research interests include high power millimeter-wave and THz vacuum tubes, quasi-optical waveguides, antennas, transmission lines, and various applications using high power millimeter-wave and THz sources such as plasma heating and current drive, plasma diagnostics, and breakdown.

Neville C. Luhmann, Jr., Dept. of Electrical and Computer Engineering, UC Davis Distinguished Professor, APS Fellow, IEEE Fellow, recipient of the IEEE John R. Pierce award for Excellence in Vacuum Electronics, the Kenneth J. Button Award for "Recognition of Outstanding Contributions to the Science of the Electromagnetic Spectrum," the Plasma Science and Applications Committee Award for "Outstanding Contributions to the Field of Plasma Science" 2005, and recipient of the Robert L. Woods Award, Award for "Excellence in Vacuum Electronics" given by the Office of the Secretary of Defense.